![Chalmers University of Technology logo]

Dynasor - A Tool for Extracting Dynamical Structure Factors and Current Correlation Functions from Molecular Dynamics Simulations

(article starts on next page)

DYNASOR—A Tool for Extracting Dynamical Structure Factors and Current Correlation Functions from Molecular Dynamics Simulations

Erik Fransson, Mattias Slabanja, Paul Erhart,* and Göran Wahnström*

Perturbative treatments of the lattice dynamics are widely successful for many crystalline materials; however, their applicability is limited for strongly anharmonic systems, metastable crystal structures and liquids. The full dynamics of these systems can, however, be accessed via molecular dynamics (MD) simulations using correlation functions, which includes dynamical structure factors providing a direct bridge to experiment. To simplify the analysis of correlation functions, here the DYNASOR package is presented as a flexible and efficient tool that enables the calculation of static and dynamical structure factors, current correlation functions as well as their partial counterparts from MD trajectories. The DYNASOR code can handle input from several major open source MD packages and thanks to its C/Python structure can be readily extended to support additional codes. The utility of DYNASOR is demonstrated via examples for both solid and liquid single and multi-component systems. In particular, the possibility to extract the full temperature dependence of phonon frequencies and lifetimes is emphasized.

1. Introduction

The dynamical properties of materials are fundamental to, for example, their thermodynamic, kinetic, optical and transport properties. They can be accessed via neutron[1–4] or X-ray[5] scattering experiments, which provide quantitative information in the form of dynamical structure factors.[6,7] The latter can also be generated using atomic scale modeling via molecular dynamics (MD) simulations or lattice dynamics, providing a quantitative bridge between experiment and atomic scale modeling.

MD simulations are the primary choice for modeling liquids[8] and in recent years several packages geared toward the analysis of their dynamics have emerged, including, for example, NMOLDYN,[9] MDANSE,[10] LIQUIDLIB,[11] and FREUD.[12] The dynamical properties of (periodic) solid state systems are, on the other hand, commonly analyzed within the framework of lattice dynamics, that is, a low-order expansion of energy and forces in terms of small atomic displacements. The lowest (second-order) force constant (FC) expansion can be conveniently handled using packages such as PHONOPY[13] or PHONON,[14] while higher-order terms can be obtained either directly via tools such as PHONO3PY[15] and SHENGBTE[16] (for third-order FC terms) or via regression using, for example, ALAMODE,[17] TDEP,[18] CSLD[19] or HIPHIVE.[20]

The calculation of the dynamical properties in general and the dynamical structure factor in particular via the FC approach typically includes only second-order (harmonic) or third-order (lowest anharmonic order) terms, limiting the approach to materials with relatively weak anharmonicity. Moreover, the quick explosion of terms with system size imposes a rather severe limit on system size. As a result, the computation of the dynamical properties becomes very cumbersome or impossible for materials with large unit cells, low symmetry and/or strong anharmonicity, including metastable crystal structures and materials with soft modes, which exhibit particular rich and interesting dynamical properties (For lattice-based systems, phonon frequencies and lifetimes can also be obtained from MD simulations via the spectral energy density.[21,22] The latter approach, however, breaks down for amorphous structures and solids that exhibit diffusion.).

All of the latter limitations can in principle be overcome by analyzing correlation functions, such as the dynamical structure factor, from MD simulations using forces from density-functional theory (DFT) calculations, empirical potentials[23] or high-order force constants.[24] To take full advantage of this approach it is desirable to obtain the dispersion relations as a function of not only the magnitude but also the direction of the momentum transfer vector. While this information is in principle present whenever analyzing trajectories from periodic systems, this is not the primary focus of the aforementioned tools. Here, to fill this need, we introduce the DYNASOR package for the efficient calculation of dynamical structure factors from MD trajectories. While it is generally applicable to both solids and liquids, it is particularly well suited to analyze the dynamics of fully or partially periodic systems.

DYNASOR, which is written in a combination of C and Python, can parse MD trajectories from LAMMPS,[23] GROMACS[25] as well as NAMD.[26] If VMD[27] is available, DYNASOR can employ the

E. Fransson, M. Slabanja, Prof. P. Erhart, Prof. G. Wahnström
Department of Physics
Chalmers University of Technology
S-412 96 Gothenburg, Sweden
E-mail: erhart@chalmers.se; goran.wahnstrom@chalmers.se

**ADVANCED
SCIENCE NEWS**

www.advancedsciencenews.com

**ADVANCED
THEORY AND
SIMULATIONS**

www.advtheorysimul.com

molfileplugin to read even more formats (with some limitations). By using existing trajectory converters such as MDTRAJ[28] and PIZZA[29] as well as tools such as ASE,[30] it is straightforward to parse many more formats, including those from ab-initio MD simulations. The code then allows one to compute not only the dynamical structure factor but also current correlation as well as partial correlation functions. In this fashion, it is for example possible to extract the full temperature dependence of phonon dispersions, as illustrated below for both solids (Sections 4.1 and 4.3) and liquids (Sections 4.2 and 4.4).

Below, we first provide a review of the theoretical background, before describing the implementation and basic usage of DYNASOR. We then demonstrate the application and performance of the code for both solids and liquids, and specifically illustrate the extraction of phonon dispersions and lifetimes.

2. Theoretical Background

In the following we provide a concise compilation of the expressions for the dynamical structure factor and current correlation functions in terms of the atomic coordinates and velocities. More extensive information can be found, for example, in refs. [7] and [31]. We describe a theoretical framework for how these correlation functions can be analyzed in order to extract vibrational information of the system.

2.1. Dynamical Structure Factor

The density of atoms $n(\mathbf{r}, t)$ is defined as

$$n(\mathbf{r}, t) = \sum_i^N \delta(\mathbf{r} - \mathbf{r}_i(t)), \tag{1}$$

where $\mathbf{r}_i(t)$ denotes the position of atom i at time t and N is the total number of atoms. The density can be spatially Fourier transformed via

$$n(\mathbf{q}, t) = \int n(\mathbf{r}, t) e^{i\mathbf{q}\cdot\mathbf{r}} d\mathbf{r} = \sum_i^N e^{i\mathbf{q}\cdot\mathbf{r}_i(t)} \tag{2}$$

The intermediate scattering function $F(\mathbf{q}, t)$ is defined in terms of the time correlation function of $n(\mathbf{q}, t)$ as

$$F(\mathbf{q}, t) = \frac{1}{N} \langle n(\mathbf{q}, t)n(-\mathbf{q}, 0) \rangle, \tag{3}$$

where $< \dots >$ denotes an ensemble average or —if the systems is ergodic— a time average. The static structure factor is given by the initial value of the intermediate scattering function

$$S(\mathbf{q}) = F(\mathbf{q}, t = 0), \tag{4}$$

while one obtains the dynamical structure factor $S(\mathbf{q}, \omega)$ via a temporal Fourier transformation of $F(\mathbf{q}, t)$

$$S(\mathbf{q}, \omega) = \int_{-\infty}^{\infty} F(\mathbf{q}, t) e^{-i\omega t} dt. \tag{5}$$

$S(\mathbf{q}, \omega)$ exhibits peaks in the $(\mathbf{q}, \omega)$ plane corresponding to longitudinal modes. The broadening of these peaks is related to the phonon lifetimes and thus the anharmonicity of the system (Section 4.1).

2.2. Velocity Autocorrelation Function

The velocity autocorrelation function (VACF), $\Phi(t)$, is defined as

$$\Phi(t) = \frac{1}{N} \sum_i^N \frac{\langle \mathbf{v}_i(t) \cdot \mathbf{v}_i(0) \rangle}{\langle \mathbf{v}_i(0) \cdot \mathbf{v}_i(0) \rangle}, \tag{6}$$

where $v_i(t)$ denotes the velocity of atom i at time t. The Fourier transformation of $\Phi(t)$ is related to the vibrational density of states, $g(\omega)$, via

$$g(\omega) = \frac{2}{\pi} \int_0^{\infty} \Phi(t) \cos(\omega t) dt \tag{7}$$

2.3. Current Correlations

In order to obtain mode specific vibrational frequencies the positions of the atoms need to be included in the analysis. This can be done by computing current correlation functions. These are defined in a fashion that is analogous to the approach for the intermediate scattering function, but with the atom density being replaced with the current density, $n(\mathbf{r}, t)$,

$$\mathbf{j}(\mathbf{r}, t) = \sum_i^N \mathbf{v}_i(t)\delta(\mathbf{r} - \mathbf{r}_i(t))$$

$$\mathbf{j}(\mathbf{q}, t) = \sum_i^N \mathbf{v}_i(t) e^{i\mathbf{q}\cdot\mathbf{r}_i(t)}. \tag{8}$$

The current density is a vector quantity which can be decomposed into a longitudinal part containing the component parallel to the $\mathbf{q}$-vector and a transverse part containing the perpendicular component, according to

$$\mathbf{j}(\mathbf{q}, t) = \mathbf{j}_L(\mathbf{q}, t) + \mathbf{j}_T(\mathbf{q}, t) \tag{9}$$

where

$$\mathbf{j}_L(\mathbf{q}, t) = \sum_i^N (\mathbf{v}_i(t) \cdot \hat{\mathbf{q}})\hat{\mathbf{q}} e^{i\mathbf{q}\cdot\mathbf{r}_i(t)}$$

$$\mathbf{j}_T(\mathbf{q}, t) = \sum_i^N \left[\mathbf{v}_i(t) - (\mathbf{v}_i(t) \cdot \hat{\mathbf{q}})\hat{\mathbf{q}} \right] e^{i\mathbf{q}\cdot\mathbf{r}_i(t)} \tag{10}$$

and $\hat{\mathbf{q}}$ denotes the unit vector. The current correlation functions can now be computed (analogous to the intermediate scattering function) as

$$C_L(\mathbf{q}, t) = \frac{1}{N} \langle \mathbf{j}_L(\mathbf{q}, t) \cdot \mathbf{j}_L(-\mathbf{q}, 0) \rangle$$

$$C_T(\mathbf{q}, t) = \frac{1}{N} \langle \mathbf{j}_T(\mathbf{q}, t) \cdot \mathbf{j}_T(-\mathbf{q}, 0) \rangle. \tag{11}$$

**ADVANCED
SCIENCE NEWS**
www.advancedsciencenews.com

**ADVANCED
THEORY AND
SIMULATIONS**
www.advtheorysimul.com

As in the case of the intermediate scattering function, the current correlations can be temporally Fourier transformed to the frequency domain. By inspection of (2) and (3) particle density and current density are related via

$$\frac{\partial}{\partial t} n(\mathbf{q}, t) = \mathrm{i}\mathbf{q} \cdot \mathbf{j}(\mathbf{q}, t), \tag{12}$$

which yields the following relation

$$\omega^2 S(\mathbf{q}, \omega) = q^2 C_L(\mathbf{q}, \omega) \tag{13}$$

in the frequency domain.

2.4. Multi-Component Systems and Liquids

In multi-component systems one can furthermore introduce partial correlation functions. For example in the case of a binary system (AB) the above expressions for the particle density generalize to

$$n_A(\mathbf{q}, t) = \sum_i^{N_A} \mathrm{e}^{\mathrm{i}\mathbf{q} \cdot \mathbf{r}_i(t)}$$

$$F_{AB}(\mathbf{q}, t) = \frac{1}{\sqrt{N_A N_B}} \langle n_A(\mathbf{q}, t) n_B(-\mathbf{q}, 0) \rangle. \tag{14}$$

This generalization extends to current correlations in the same manner. In some situations, instead of analyzing the partial correlation functions directly, it is convenient to consider linear combinations of these functions. This will be demonstrated and discussed in the case of liquid NaCl in Section 4.4.

In solids, it is often desirable to determine the above mentioned quantities along specific paths connecting high symmetry **q**-points. In isotropic samples on the other hand, such as for example liquids, it is usually preferable to compute these functions with respect to $q = |\mathbf{q}|$, by performing a spherical average.

2.5. Damped Harmonic Oscillators—Fitting

Phonons are often modeled as damped harmonic oscillators.[1,32] This enables correlation functions from both experiments and computer simulations to be fitted to the corresponding analytic functions, allowing the extraction of phonon frequency and lifetime (or damping factor). For this purpose, the analytic form for the above mentioned correlation functions is derived and analyzed in the following.

Assuming the particle density, $n(\mathbf{q}, t)$, oscillates as a damped harmonic oscillator then $F(\mathbf{q}, t)$ is, for each **q**, described by a function $a(t)$ that is given by

$$\frac{\mathrm{d}^2}{\mathrm{d}t^2} a(t) + \Gamma \frac{\mathrm{d}}{\mathrm{d}t} a(t) + \omega_0^2 a(t) = 0, \tag{15}$$

where Γ is the damping coefficient and ω_0 the natural frequency of the oscillator. This means that $\Gamma = \Gamma(\mathbf{q})$ and $\omega_0 = \omega_0(\mathbf{q})$, but for simplicity these arguments are left out through out the rest of this section. This equation is solved under the assumptions

that $\frac{\mathrm{d}}{\mathrm{d}t} a(t = 0) = 0$ and $t \geq 0$. For simplicity we set $a(t = 0) = A$ yielding the following solution

$$F(t) = A\mathrm{e}^{-\Gamma t/2} \left(\cos \omega_e t + \frac{\Gamma}{2\omega_e} \sin \omega_e t \right), \ \omega_0 > \frac{\Gamma}{2}$$
$$F(t) = A\mathrm{e}^{-\Gamma t/2} \left(\cosh \omega_e t + \frac{\Gamma}{2\omega_e} \sinh \omega_e t \right), \ \omega_0 < \frac{\Gamma}{2}, \tag{16}$$

where $\omega_e = \sqrt{\omega_0^2 - \frac{\Gamma^2}{4}}$ and $\omega_0 > \frac{\Gamma}{2}$ represents the underdamped limit. This yields three fitting parameters A, Γ, and ω_0 for each **q**. The functional form for $a(t)$ can be Fourier transformed to

$$a(\omega) = A \frac{2\Gamma \omega_0^2}{(\omega^2 - \omega_0^2)^2 + (\Gamma \omega)^2}. \tag{17}$$

This corresponds to the analytic functional form of the dynamical structure factor, which is thus a peaked function with a maximum at $\omega_{max} = \sqrt{\omega_0^2 - \frac{\Gamma^2}{2}}$ and full-width-at-half-maximum FWHM $\approx \Gamma$.

This analysis can be extended to current correlation functions by considering (4), giving the following solutions

$$b(\omega) = B \frac{2\Gamma \omega^2}{(\omega^2 - \omega_0^2)^2 + (\Gamma \omega)^2}. \tag{18}$$

This is a peaked function with a maximum at $\omega_{max} = \omega_0$ and full-width-at-half-maximum FWHM $\approx \Gamma$. In the time domain this function becomes

$$b(t) = B\mathrm{e}^{-\Gamma t/2} \left(\cos \omega_e t - \frac{\Gamma}{2\omega_e} \sin \omega_e t \right), \ \omega_0 > \frac{\Gamma}{2}$$
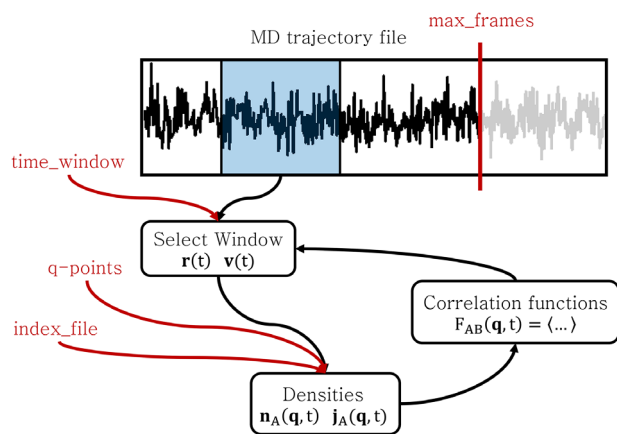$$b(t) = B\mathrm{e}^{-\Gamma t/2} \left(\cosh \omega_e t - \frac{\Gamma}{2\omega_e} \sinh \omega_e t \right), \ \omega_0 < \frac{\Gamma}{2} \tag{19}$$

with three fit parameters B, Γ, and ω_0. While these expressions are strictly valid for the longitudinal current correlations, we assume the same functional form also when fitting the transverse components. Since there are two transverse modes a sum of two functions is needed (unless the transverse mode is degenerate), giving us six fit parameters instead of three. The damping coefficient Γ is related to the phonon lifetime (also referred to as relaxation or scattering time) τ as $\tau = 2/\Gamma$.

2.6. Fourier Transforms

It is often desirable to transform time dependent correlation functions to the frequency domain. There are many different methods for carrying out numerical Fourier transforms, window functions can be applied and the signal can be zero padded to obtain better accuracy. Since all time-dependent functions are included in the output from DYNASOR it is therefore possible to carry out the Fourier transform in any which way. By default DYNASOR will provide correlation functions also in the frequency domain using Filon's formula to carry out the transform as described in appendix D of ref. [8]. We note that using window functions such as a Fermi–Dirac function

$$h(t) = \frac{1}{\mathrm{e}^{(t-t_0)/t_{width}} + 1} \tag{20}$$

**ADVANCED
SCIENCE NEWS**

www.advancedsciencenews.com

**ADVANCED
THEORY AND
SIMULATIONS**

www.advtheorysimul.com

Figure 1. Internal workflow of DYNASOR. Text in red marks user inputs. The time window, indicated in blue, is moved through the trajectory until the specified maximum number of frames is reached.

works very well for preserving the important features but reduces the noise in the correlation functions. Here, t_0 and t_{width} are parameters that should be suitably chosen, given the relaxation time of the correlation function.

3. Software Details

DYNASOR is distributed under on open source software license (MIT) and its development is hosted on GITLAB.[33] A comprehensive documentation written in SPHINX[34] is included in the distribution and is also available online.[35] Below some implementation aspects and inner workings of DYNASOR are outlined.

The workflow of DYNASOR is illustrated in **Figure 1**. The collection of snapshots corresponding to a time window is parsed from the MD trajectory, and for each snapshot the densities are computed and then the correlation functions. This process is repeated until there are no more snapshots left in the trajectory or the limit of numbers of snapshots to consider is met.

DYNASOR can read and parse trajectories in LAMMPS dump format. If the LIBGMX library from the GROMACS package is available, DYNASOR can also read GROMACS xtc-files. If VMD is installed,[27] DYNASOR can use the MOLFILE plugin to read other formats (with some limitations) as well.

The time sampling can be adjusted via input parameters such as the size of time window and the maximum number of snapshots to consider. **q**-point sampling is configured via four different parameters, controlling sampling style (isotropic or along a path), the maximum **q**-vector to include, and the number of **q**-points/**q**-bins. For multi-component systems an index file (`index_file`) must be provided, indicating which atomic indices corresponds to which atom types. For more details about these input parameters see the DYNASOR documentation or examples.[35]

The output data from DYNASOR consists of

- Partial intermediate scattering function $F(\mathbf{q}, t)$
- Partial dynamical structure factor $S(\mathbf{q}, \omega)$
- Partial longitudinal and transverse partial current correlations $C(\mathbf{q}, t)$ and $C(\mathbf{q}, \omega)$
- Partial van Hove function $G(\mathbf{r}, t)$

- Partial self part of $F(\mathbf{q}, t)$ and $S(\mathbf{q}, \omega)$

This collection of data can be written as Python pickle-files or MATLAB/OCTAVE .m files.

The computationally most demanding task in the process pipeline, concerns the calculation of the Fourier transformed densities, $n(\mathbf{q}, t)$ and $\mathbf{j}(\mathbf{q}, t)$. This part is implemented in C and is accelerated by parallelization using OPENMP[36] or OPENACC.[37] Once the densities have been computed the averaging of the time correlations is performed in Python.

4. Applications

We now turn to exemplary applications of DYNASOR to "real" materials and illustrate the information available in the correlation functions for different systems. In all cases described below MD simulations were carried out using the LAMMPS package.[23] Following equilibration in either the canonical (*NVT*) or isothermal-isobaric (NPT) ensemble using the Nosé–Hoover thermostat and/or barostats, positions and velocities were sampled for about one nanosecond in the microcanonical (NVE) ensemble in order to avoid the thermostat/barostat influencing the dynamics and thus the correlation functions.

When showing dispersion relations, we chose to plot ω_0, rather than ω_e, unless explicitly noted. The difference between ω_0 and ω_e is often small, but for system with strong damping there is a clear difference as shall be discussed in the case of body-centered cubic (BCC)-Ti (Section 4.3).
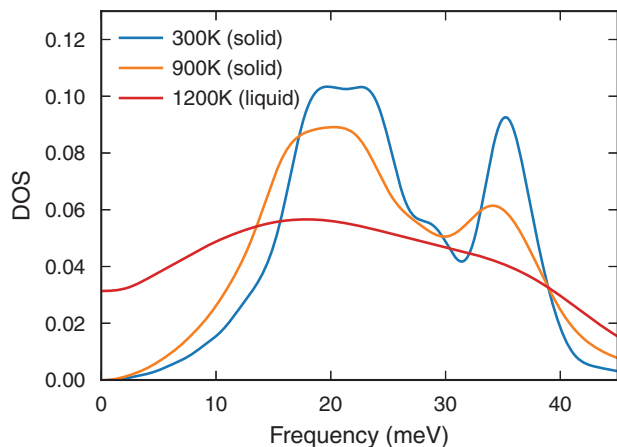
4.1. Solid (FCC) Aluminum

We first consider face-centered cubic (FCC)-Al since it is a rather harmonic system, for which we can carry out meaningful comparisons with perturbative methods.

The atomic interactions in aluminum were modeled using an embedded atom method potential for[38] and simulations were carried out at 300 and 900 K using a supercell comprising $12 \times 12 \times 12$ conventional face-centered cubic unit cells. Frequencies and lifetimes can be affected by finite-size effects.[39] We therefore checked the convergence of our data by also analyzing smaller supercells down to $4 \times 4 \times 4$ unit cells and found frequencies and damping in the present case to vary by less than 0.05 meV at 300 K.

A comparison of the density of states (DOS) for FCC and liquid Al (to be described in more detail in Section 4.2), computed via Equation (2), shows obvious qualitative differences between the solid and liquid phases (**Figure 2**). The DOS in the solid phase vanishes at zero frequency and shows softening with increasing temperature. By contrast the liquid DOS is finite at zero frequency corresponding to diffusive motion while still exhibiting structure at nonzero frequencies resembling solid behavior.

The phonon frequencies and lifetimes were extracted at a fixed lattice parameter, $a = 4.05$Å, across the entire temperature range in order to enable comparison with results from the harmonic approximation and first-order perturbation theory. The current correlation functions were calculated and fitted in the time domain using the procedure outlined in Section 2.5 using Equation (5)

ADVANCED
SCIENCE NEWS
www.advancedsciencenews.com

ADVANCED
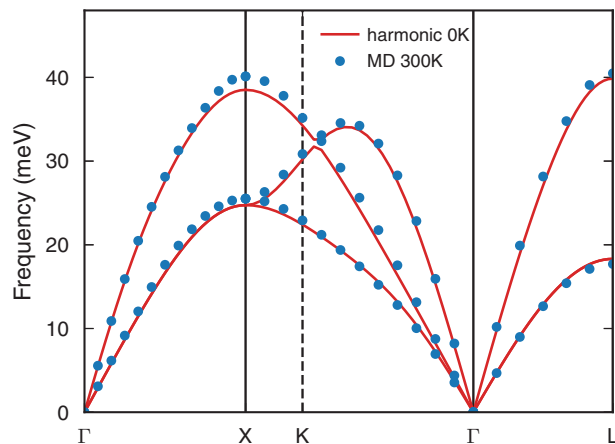**THEORY AND**
SIMULATIONS
www.advtheorysimul.com

Figure 2. Vibrational density of states for aluminum at 300 K (solid), 900 K (solid), and 1200 K (liquid), computed from the velocity autocorrelation function.
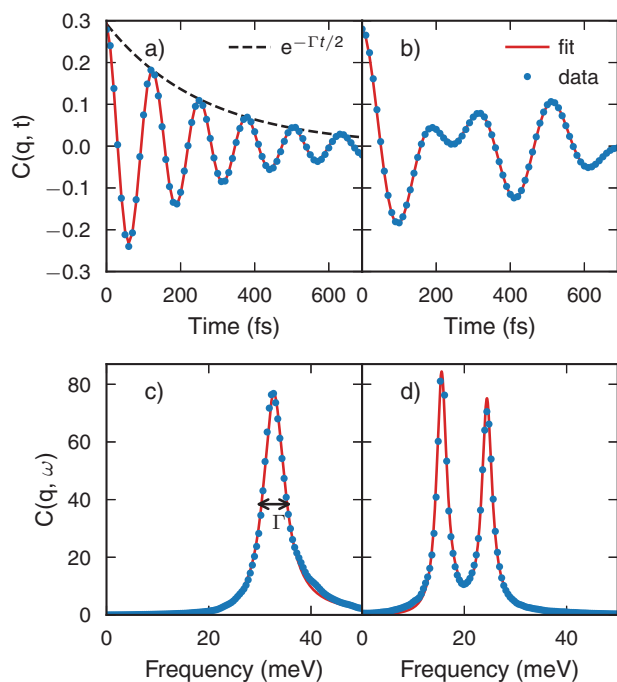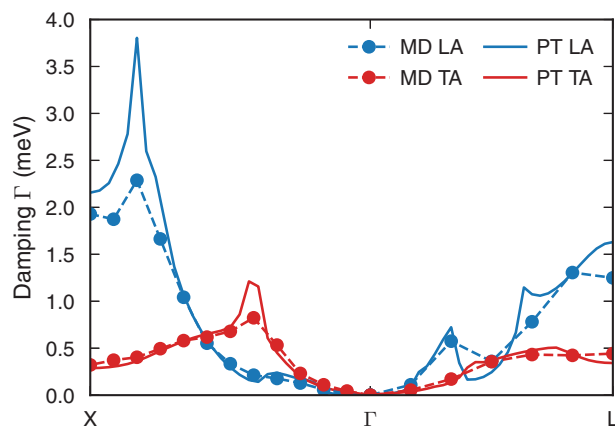

Figure 3. Solid (FCC) aluminum at 900 K. Fits for the a) longitudinal and b) transverse current correlations in the time domain for a **q**-point halfway along the $\Gamma - K - X$ path. The corresponding functions in the frequency domain are shown for the c) longitudinal and d) transverse current correlation functions.

Figure 4. Phonon dispersion of solid (FCC) aluminum from MD simulations at 300 K and in the harmonic (0 K) approximation.

Figure 5. Phonon damping (inverse lifetime) in solid (FCC) aluminum at 300 K from MD simulations (via DYNASOR) and first-order perturbation theory (PT) via PHONO3PY.

the present case, the phonon dispersion at 300 K closely agrees with the harmonic (zero Kelvin) phonon dispersion obtained via PHONOPY,[13] as expected given the weak anharmonicity in FCC-Al.
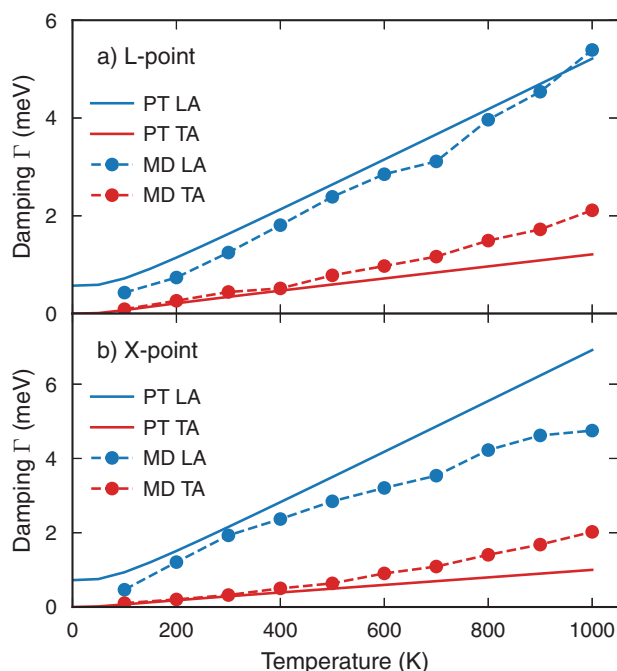
The phonon lifetimes calculated using DYNASOR and PHONO3PY are shown along $\Gamma - X$ and $\Gamma - L$ at 300 K in **Figure 5**. Here, Γ obtained from DYNASOR by fitting to Equation (5) is shown together with the damping obtained from PHONO3PY. The latter has been multiplied by a factor of four to accommodate the different definitions. The phonon lifetime is given by

$$\tau = \frac{2}{\Gamma_{\text{dynasor}}} = \frac{1}{2\Gamma_{\text{phono3py}}} \tag{21}$$

and hence for consistency we compare Γ_{dynasor} with $4\Gamma_{\text{phono3py}}$.

The lifetimes are long, consistent with weak anharmonicity. The agreement between DYNASOR and PHONO3PY is good, both qualitatively and quantitatively. This is expected for low temperatures where first-order perturbation theory captures most of the relevant anharmonic contributions to the lifetimes. As temperature increases higher-order terms become increasingly

for both the longitudinal and transverse current correlation functions (**Figure 3**). The representation via the analytical functions in the frequency domain also matches the Fourier transformed data very well, providing further validation of the approach. While fitting in the time domain is often easier when dealing with few modes, the frequency domain becomes preferable when many modes are present since they are more clearly separated along the ω axis.

By extending the fitting procedure to all **q**-points in the supercell, one obtains the full phonon dispersion (**Figure 4**). In

**ADVANCED
SCIENCE NEWS**

www.advancedsciencenews.com

**ADVANCED
THEORY AND
SIMULATIONS**

www.advtheorysimul.com

Figure 6. Phonon damping (inverse lifetime) in solid aluminum from MD simulations (via DYNASOR) and first-order perturbation theory (PT), via PHONO3PY, for the LA and TA modes at a) L and b) X as a function of temperature.

important and the lifetimes obtained via first-order perturbation theory deviate more and more strongly from those obtained from MD simulations, which include scattering to all orders (**Figure 6**).

One might intuitively expect the inclusion of higher-order FC terms to lead to a systematic increase in damping (equivalent to a shortening of the lifetimes). The comparison between PHONO3PY and the MD results, however, shows for some modes the opposite behavior. This can be explained by recalling that scattering also leads to a shift of the frequencies with temperature, which changes the geometry of the scattering events, making it difficult to develop a simple intuitive picture for the sign of the change. We also note that while the difference between a perturbative and a self-consistent treatment of the lifetimes is small in Al due to its low degree of anharmonicity, it is often much more pronounced in strongly anharmonic systems as shown explicitly in, for example, refs. [40,41].

4.2. Liquid Aluminum

To illustrate the application of DYNASOR for analyzing liquid phases, we now consider liquid aluminum, which was simulated using the same potential as for its solid counterpart[38] and using the same number of atoms (6912). We carried out simulations at 1200 K with isotropic **q**-space sampling, yielding a structure factor (**Figure 7**a) in good agreement with literature data.[42] To illustrate the calculated intermediate scattering function, $F(q, t)$, and dynamical structure factor, $S(q, \omega)$, two slices are shown for $q = 5.05 \, \mathrm{nm}^{-1}$ and $q = 9.90 \, \mathrm{nm}^{-1}$ in Figure 7b,c). The behavior

observed corresponds to a diffusion (gas-like) part and a vibrational (solid-like) part[43] In the time domain this corresponds to a decaying function and damped oscillator function, respectively, whereas in the frequency domain it corresponds to a decaying function that is nonzero at $\omega = 0$ and a peak function, respectively.

The full $q - \omega$ plane is visualized in **Figure 8** for $S(q, \omega)$, $C_L(q, \omega)$ and $C_T(q, \omega)$. Clear dispersion relations can be observed, which are in agreement with both experimental measurements and computer simulations.[42] We note that the longitudinal dispersion, which can be seen in both $S(q, \omega)$ and $C_L(q, \omega)$, is more distinct in the latter as it does not contain the diffusive (gas-like) part. Since resolution deteriorates for very low q-values, due to the finite size of the MD simulation, the x-axis has been cut at $q = 2.5 \, \mathrm{nm}^{-1}$.

4.3. BCC Titanium

Having established the basic procedure for analyzing phonon dispersion and lifetimes for a rather harmonic system such as FCC-Al, we can now turn to a material, for which perturbative analyses fail altogether, namely the BCC phase of titanium. While this phase is the most stable for temperatures between 1155 and 1943 K, the BCC structure is dynamically unstable at zero Kelvin, leading to harmonic phonon modes with imaginary frequencies. BCC-Ti therefore provides a particular interesting test case with very pronounced anharmonicity and a strongly temperature dependent phonon dispersion that has already been extensively investigated experimentally.[1] The modes for which these effects are most pronounced are related to the BCC-hexagonal-closed packed (HCP) (TA1 at N-point) and the BCC-ω transition (LA along H-P direction).[1] Further, BCC-Ti exhibits spontaneous defect formation and migration,[44] which complicates its analysis with lattice dynamics approaches.

The atomic interactions were described using a modified embedded-atom-method potential,[45] which accurately reproduces the different phases. MD simulations were carried out using $12 \times 12 \times 12$ conventional BCC unit cells. The system was first equilibrated in isothermal-isobaric (NPT) ensemble in order to obtain the correct lattice parameter after which the correlation functions were sampled in the microcanonical (NVE) ensemble.

Extraction of the phonon dispersion and lifetimes proceeded in the same fashion as for the case of FCC-Al. As a result of the strong anharmonicity the correlation functions exhibit, however, much more asymmetric shapes that clearly deviate from simple Lorentzian line shapes. The phonon dispersion at 1400 K (in the middle of the stability range of the BCC phase) clearly shows this strong damping, especially near the N-point and along the H-P direction (**Figure 9**a). The comparison with the harmonic dispersion further demonstrates the strong renormalization of the phonon modes by temperature, which not only leads to very pronounced shifts in the frequencies but also affects the shape of the dispersion, as is most apparent for the lower transverse acoustic (TA) mode along the H-P direction.

Given the importance of the TA1 mode at the N-point for the BCC-HCP transition,[1] we analyzed the temperature dependence of the transverse current correlation function at this point
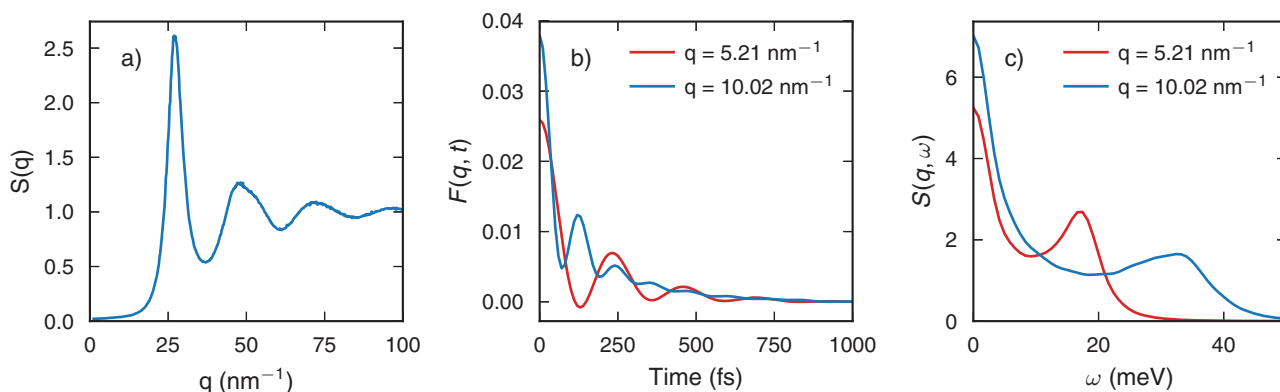
Figure 7. Liquid aluminum at 1200 K. a) Structure factor, b) intermediate scattering function, $F(q, t)$, and c) the dynamical structure factor, $S(q, \omega)$.
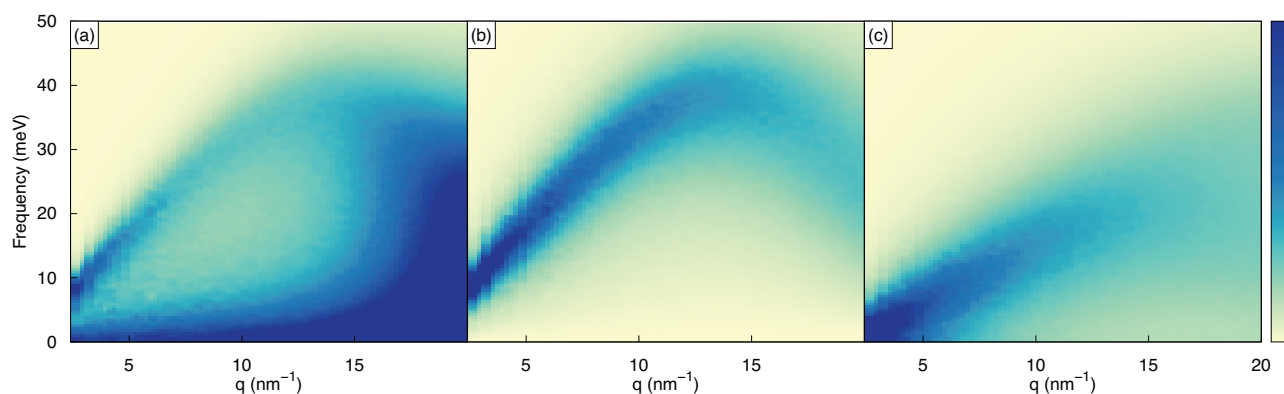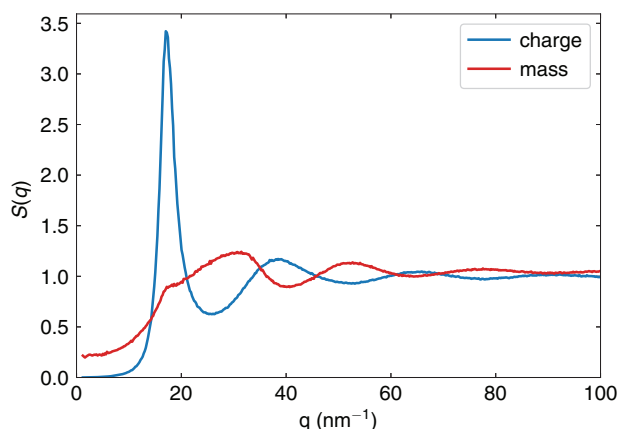

Figure 8. Liquid aluminum at 1200 K. a) Dynamical structure factor, b) longitudinal current, and c) transverse current as a function of q and ω. **q**-vectors are cut below 2.5 nm⁻¹ due to the poor resolution beyond that point.
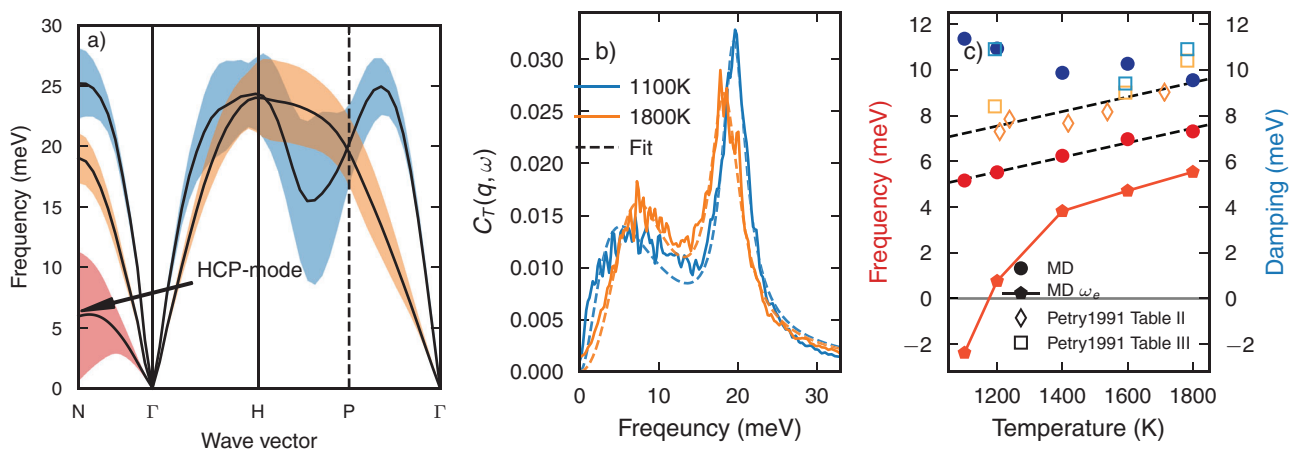
Figure 9. a) Phonon dispersion relation for BCC Ti at 1400 K obtained from MD simulations. The shaded regions indicate the phonon lifetimes. b) The transverse current correlation at the N-point, and corresponding fits as dashed lines, at 1100 K and 1800 K. c) Frequency and damping of the lower most TA mode at the N-point, corresponding to the BCC→HCP transition, as a function of temperature. The frequencies are given in red/orange and damping coefficients in blue. Here, results from inelastic neutron measurements[1] and DYNASOR analysis are shown by open markers and filled markers, respectively. The frequency ω_e becomes imaginary (drawn as negative) at around 1200 K indicating that the mode is overdamped. Dashed black lines are drawn as a guide to the eye to show the linear decrease of the frequency as temperature decreases.

**ADVANCED
SCIENCE NEWS**
www.advancedsciencenews.com

**ADVANCED
THEORY AND
SIMULATIONS**
www.advtheorysimul.com

Figure 10. Charge and mass structure factor for liquid sodium chloride at 1200 K.

in more detail (Figure 9b). The results agrees very well with experimental work[1] both with respect to slope and absolute magnitude (Figure 9c). This illustrates how the dynamics of strongly anharmonic modes in the strongly and over-damped limits can be readily extracted using DYNASOR. The analysis also clarifies the distinction between ω_e and ω_0 that becomes apparent for strongly damped modes.

4.4. Liquid Sodium Chloride

Lastly a liquid two-component system, molten sodium chloride (NaCl), is studied in order to illustrate how the partial correlation functions can be used. Some useful linear combinations of the partial correlation functions are the charge and mass correlation,

defined as

$$S_{\text{charge}}(q, \omega) = \sum_i \sum_j Q_i Q_j S_{ij}(q, \omega) \Big/ \sum_i \sum_j |Q_i Q_j|$$

$$S_{\text{mass}}(q, \omega) = \sum_i \sum_j m_i m_j S_{ij}(q, \omega) \Big/ \sum_i \sum_j m_i m_j$$

(22)

where i, j represent the atom types, m_i and Q_i are respectively mass and charge of species i. These linear combination are possible not only for $S(q, \omega)$ but for all correlation functions in both frequency and time domain. Commonly acoustic type modes are revealed in mass-mass correlations whereas charge-charge correlation can be used to investigate optical modes.

A Born–Mayer–Huggins style potential was used together with a Coulombic term as implemented in the pair style born/coul/long in LAMMPS[23] with the parameters reported by Lewis and Singer.[46] MD simulation were first carried out in the NPT and then the NVE ensemble for systems comprising 4096 atoms at 1200 K.

The static charge and mass structure factor is shown in **Figure 10**. The charge and mass current correlations computed from (8) are visualized in the $q - \omega$ space in **Figure 11**. In the charge correlation function a clear longitudinal and a weak transverse optical mode are visible, while in the mass correlation function the acoustic modes can be seen.

5. Conclusions

In this paper, we have presented the DYNASOR package, which is designed to aid in the analysis of dynamical correlation functions in particular in fully or partially crystalline systems, although it is equally applicable to fully disordered systems. We have demonstrated its usage via a few simple examples, including monoelemental solids and liquids as well as a two component liquid.
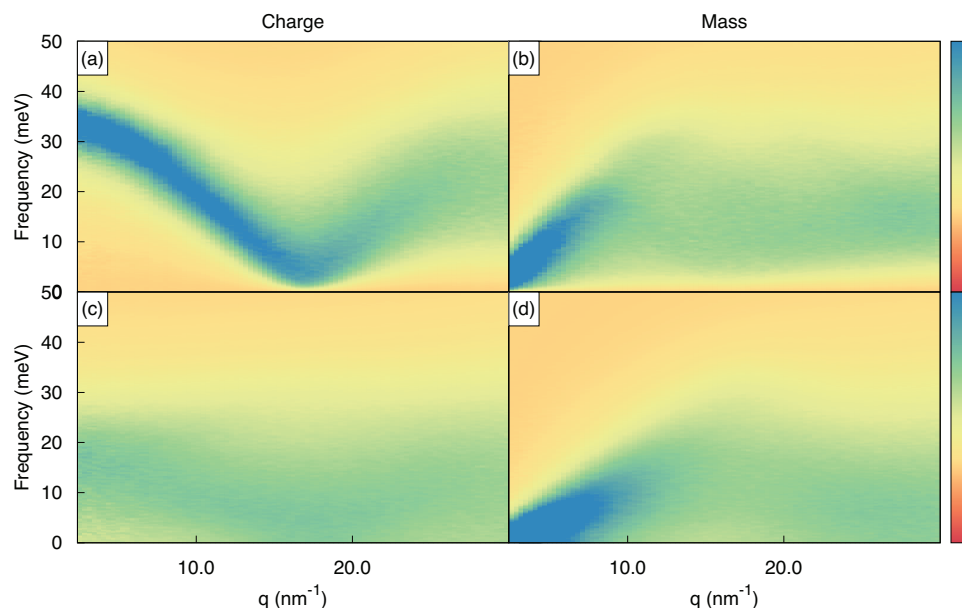
Figure 11. a,c) Charge and b,d) mass longitudinal (top) and transverse (bottom) current correlations for liquid sodium chloride at 1200 K. q-points are cut below 2.5 nm^{-1} due to the poor resolution beyond that point.

**ADVANCED
SCIENCE NEWS**

www.advancedsciencenews.com

**ADVANCED
THEORY AND
SIMULATIONS**

www.advtheorysimul.com

For all these systems, current-correlation functions are shown to be very effective for analyzing the dynamics and for extracting properties such as phonon frequencies and lifetimes.

In the case FCC-Al, for which direct comparison with standard lattice dynamical analysis techniques is possible, we demonstrate excellent agreement at low temperatures for both frequencies and lifetimes. At higher temperatures the deviation between MD results and perturbative treatments increases. This is a reflection of the limitations of the latter approach, which is typically terminated after the third-order[15,47] or (rarely) the fourth-order expansion term.[40,48–50] In contrast, MD simulations capture phonon processes to all orders. Thereby they yield the variation of both frequencies and lifetimes with temperature without the need to resort to further approximations.

Further, we demonstrate the extraction of the temperature dependence of phonon dispersion and lifetimes for a metastable crystalline material (BCC-Ti), for which perturbative treatments are not applicable. Here, the results show good agreement with with inelastic neutron scattering experiments.[1]

The present approach of extraction dynamical correlation functions from MD simulations via DYNASOR thus complements lattice dynamics techniques[4,15,51] and is essential, for example, when studying the vibrational properties of materials with large unit cells, low symmetry and/or strong anharmonicity, such as metastable crystals, systems with defects including surfaces and interfaces as well as amorphous and liquid systems.

Acknowledgements

Conflict of Interest

The authors declare no conflict of interest.

Keywords

[1] W. Petry, A. Heiming, J. Trampenau, M. Alba, C. Herzig, H. R. Schober, G. Vogl, *Phys. Rev. B* **1991**, *43*, 10933.

[2] M. Christensen, A. B. Abrahamsen, N. B. Christensen, F. Juranyi, N. H. Andersen, K. Lefmann, J. Andreasson, C. R. H. Bahl, B. B. Iversen, *Nat. Mater.* **2008**, *7*, 811.

[3] Y.-C. Lin, P. Erhart, M. Bettinelli, N. C. George, S. F. Parker, M. Karlsson, *Chem. Mater.* **2018**, *30*, 1865.

[4] C. W. Li, O. Hellman, J. Ma, A. F. May, H. B. Cao, X. Chen, A. D. Christianson, G. Ehlers, D. J. Singh, B. C. Sales, O. Delaire, *Phys. Rev. Lett.* **2014**, *112*, 175501.

[5] A. Q. R. Baron, *arXiv:1504.01098*, **2015**.

[6] S. W. Lovesey, *Theory of Neutron Scattering from Condensed Matter*, Vol. 1, Oxford Science Publications, Oxford **1984**.

[7] J.-P. Hansen, I. R. McDonald, *Theory of Simple Liquids*, 3rd ed., Elsevier, Amsterdam **2006**.

[8] M. P. Allen, D. J. Tildesley, *Computer Simulation of Liquids*, Oxford University Press, Oxford **1987**.

[9] T. Róg, K. Murzyn, K. Hinsen, G. R. Kneller, *J. Comput. Chem.* **2003**, *24*, 657.

[10] G. Goret, B. Aoun, E. Pellegrini, *J. Chem. Inf. Model.* **2017**, *57*, 1.

[11] N. P. Walter, A. Jaiswal, Z. Cai, Y. Zhang, *Comput. Phys. Commun.* **2018**, *228*, 209.

[12] V. Ramasubramani, B. D. Dice, E. S. Harper, M. P. Spellings, J. A. Anderson, S. C. Glotzer, *Comput. Phys. Commun.* **2020**, *254*, 107275.

[13] A. Togo, I. Tanaka, *Scr. Mater.* **2015**, *108*, 1.

[14] K. Parlinski, Z. Q. Li, Y. Kawazoe, *Phys. Rev. Lett.* **1997**, *78*, 4063.

[15] A. Togo, L. Chaput, I. Tanaka, *Phys. Rev. B* **2015**, *91*, 094306.

[16] W. Li, J. Carrete, N. A. Katcho, N. Mingo, *Comput. Phys. Commun.* **2014**, *185*, 1747.

[17] T. Tadano, Y. Gohda, S. Tsuneyuki, *J. Phys.: Condens. Matter* **2014**, *26*, 225402.

[18] O. Hellman, I. A. Abrikosov, S. I. Simak, *Phys. Rev. B* **2011**, *84*, 180301.

[19] F. Zhou, W. Nielson, Y. Xia, V. Ozoliņš, *Phys. Rev. Lett.* **2014**, *113*, 185501.

[20] F. Eriksson, E. Fransson, P. Erhart, *Adv. Theory Simul.* **2019**, *2*, 1800184.

[21] J. A. Thomas, J. E. Turney, R. M. Iutzi, C. H. Amon, A. J. H. McGaughey, *Phys. Rev. B* **2010**, *81*, 081411.

[22] Z. Ding, Q.-X. Pei, J.-W. Jiang, Y.-W. Zhang, *J. Phys. Chem. C* **2015**, *119*, 16358.

[23] S. Plimpton, *J. Comput. Phys.* **1995**, *117*, 1.

[24] E. Fransson, F. Eriksson, P. Erhart, *npj Comput. Mater.* **2020**, *6*, 135.

[25] M. J. Abraham, T. Murtola, R. Schulz, S. Páll, J. C. Smith, B. Hess, E. Lindahl, *SoftwareX* **2015**, *1–2*, 19.

[26] J. C. Phillips, R. Braun, W. Wang, J. Gumbart, E. Tajkhorshid, E. Villa, C. Chipot, R. D. Skeel, L. Kalé, K. Schulten, *J. Comput. Chem.* **2005**, *26*, 1781.

[27] Visual Molecular Dynamics, http://www.ks.uiuc.edu/Research/vmd/ (accessed: November 2020).

[28] R. T. McGibbon, K. A. Beauchamp, M. P. Harrigan, C. Klein, J. .M. Swails, C. X. Hernández, C. R. Schwantes, L.-P. Wang, T. J. Lane, V. S. Pande, *Biophys. J.* **2015**, *109*, 8.

[29] Pizza.py Toolkit, https://pizza.sandia.gov/ (accessed: November 2020).

[30] A. H. Larsen, J. J. Mortensen, J. Blomqvist, I. E. Castelli, R. Christensen, M. Dulak, J. Friis, M. N. Groves, B. Hammer, C. Hargus, E. D. Hermes, P. C. Jennings, P. B. Jensen, J. Kermode, J. R. Kitchin, E. L. Kolsbjerg, J. Kubal, K. Kaasbjerg, S. Lysgaard, J. B. Maronsson, T. Maxson, T. Olsen, L. Pastewka, A. Peterson, C. Rostgaard, J. Schiotz, O. Schütt, M. Strange, K. S. Thygesen, T. Vegge, L. Vilhelmsen, M. Walter, Z. Zeng, K. W. Jacobsen, *J. Phys.: Condens. Matter* **2017**, *29*, 27.

[31] J. P. Boon, S. Yip, *Molecular Hydrodynamics*, Dover Publications, Mineola, NY **1980**.

[32] R. Meyer, P. Entel, *Phys. Rev. B* **1998**, *57*, 5140.

[33] Materials-modeling, dynasor, https://gitlab.com/materials-modeling/dynasor/ (accessed: September 2020).

[34] Sphinx, http://www.sphinx-doc.org/ (accessed: September 2020).

[35] https://dynasor.materialsmodeling.org/ (accessed: September 2020).

[36] Open MP, https://www.openmp.org/ (accessed: September 2020).

[37] What is OpenACC?, https://www.openacc.org/ (accessed: September 2020).

[38] Y. Mishin, D. Farkas, M. J. Mehl, D. A. Papaconstantopoulos, *Phys. Rev. B* **1999**, *59*, 3393.

**ADVANCED
SCIENCE NEWS**

www.advancedsciencenews.com

**ADVANCED
THEORY AND
SIMULATIONS**

www.advtheorysimul.com

[39] Z. Zhang, Y. Ouyang, Y. Cheng, J. Chen, N. Li, G. Zhang, *Phys. Rep.* **2020**, *860*, 1.

[40] T. Tadano, S. Tsuneyuki, *Phys. Rev. Lett.* **2018**, *120*, 105901.

[41] D. O. Lindroth, J. Brorsson, E. Fransson, F. Eriksson, A. Palmqvist, P. Erhart, *Phys. Rev. B* **2019**, *100*, 045206.

[42] A. V. Mokshin, R. M. Yulmetyev, R. M. Khusnutdinov, P. Hänggi, *J. Exp. Theor. Phys.* **2006**, *103*, 841.

[43] S.-T. Lin, M. Blanco, W. A. Goddard, *J. Chem. Phys.* **2003**, *119*, 11792.

[44] E. Fransson, P. Erhart, *Acta Mater.* **2020**, *196*, 770.

[45] R. G. Hennig, T. J. Lenosky, D. R. Trinkle, S. P. Rudin, J. W. Wilkins, *Phys. Rev. B* **2008**, *78*, 054121.

[46] J. W. E. Lewis, K. Singer, *J. Chem. Soc., Faraday Trans. 2* **1975**, *71*, 41.

[47] J. M. Ziman, *Electrons and Phonons*, Clarendon Press, Oxford **1960**.

[48] T. Feng, L. Lindsay, X. Ruan, *Phys. Rev. B* **2017**, *96*, 161201.

[49] F. Tian, B. Song, X. Chen, N. K. Ravichandran, Y. Lv, K. Chen, S. Sullivan, J. Kim, Y. Zhou, T.-H. Liu, M. Goni, Z. Ding, J. Sun, G. A. G. U. Gamage, H. Sun, H. Ziyaee, S. Huyan, L. Deng, J. Zhou, A. J. Schmidt, S. Chen, C.-W. Chu, P. Y. Huang, D. Broido, L. Shi, G. Chen, Z. Ren, *Science* **2018**, *361*, 582.

[50] T. Tadano, S. Tsuneyuki, *Phys. Rev. B* **2015**, *92*, 054301.

[51] L. T. Kong, *Comput. Phys. Commun.* **2011**, *182*, 2201.